

STUDIES ON SOOTBLOWER JET DYNAMICS AND ASH DEPOSIT REMOVAL IN INDUSTRIAL BOILERS

Ameya Pophali^a, Babak Emami^a, Markus Bussmann^b, and Honghi Tran^{a*}

^aUniversity of Toronto
Dept. of Chemical Eng. & Applied Chemistry, 200 College St.
Toronto ON M5S 3E5
Canada

^bUniversity of Toronto
Dept. of Mechanical & Industrial Eng., 5 King's College Rd.
Toronto ON M5S 3G8
Canada

ameya.pophali@utoronto.ca
bemami@mie.utoronto.ca
bussmann@mie.utoronto.ca
honghi.tran@utoronto.ca
*corresponding author
Tel.: 1 (416) 978 8585
Fax: 1 (416) 971 2106

ABSTRACT

Sootblowers used to control deposit accumulation on boiler tubes consume substantial amounts of costly high pressure steam; this cost motivates the study of sootblowers and development of improved sootblowing strategies. This paper reviews recent research done on sootblowing at the University of Toronto on three fronts. First, the breakup behaviour of brittle deposits impacted by a supersonic gas jet was experimentally studied. Results reveal that crack formation is vital to deposit breakup: to effectively break a deposit, the jet must drill into the deposit and crack it in the short time that the deposit is exposed to the jet. Second, the interactions between a supersonic jet and various tube geometries were visualized to understand sootblower jet flow between boiler tube bundles. Images show that sootblower jet flow and penetration between platens is strongly affected by any interaction between the jet and the first tube of the platen. Finally, a CFD model of a turbulent supersonic sootblower jet was developed. The model yields results that are in good agreement with available laboratory and in-situ sootblower measurements.

Keywords: *sootblowing optimization, brittle deposit breakup, jet/tube interaction, off-design jets, schlieren visualization, CFD modeling.*

1.0 INTRODUCTION

A variety of fuels are burned in industrial boilers, including coal and natural gas in utility boilers, black liquor in kraft recovery boilers, biomass in biomass boilers, and municipal waste in incinerators. The fuel composition, and specifically the fuel ash content, affects the characteristics and amount of ash deposits that accumulate on boiler heat transfer surfaces, that

lower boiler thermal efficiency and in severe cases lead to boiler plugging. These problems can be exacerbated by the trend towards fuel switching, the use of boilers to burn fuel for which they were not originally designed (e.g. fuel oil, biomass, and waste gases from around a plant, in place of fossil fuels).

The usual approach to controlling deposit accumulation in nearly all boilers is the use of sootblowers that generate supersonic steam jets to knock deposits off of tubes. Sootblowing requirements vary depending on the type of boiler. In power boilers, plugging is less of a concern because deposits are not very strong and tenacious, and so sootblowers are not operated continuously. On the other hand, deposits in kraft recovery boilers are much stronger: in some locations, deposits are sticky and tenacious, but over large portions of the boiler, deposits are hard and brittle. Sootblowers are usually operated continuously (in a cycle) to ensure reliable operation of the boiler. Consequently, a substantial amount of costly high pressure steam generated by the boiler (typically between 6-10%) is used by the sootblowers, that otherwise would contribute to power generation. For a kraft recovery boiler, eliminating one sootblower that consumes 22,000 lb of steam per hour would save approximately \$1.8 million a year. As a result, optimizing sootblowing to minimize steam consumption and maximize deposit removal is important.

The effectiveness of sootblowing depends upon many factors: those that characterize the sootblower, such as steam flow rate, supply pressure, and nozzle design, and those that characterize the deposits, such as size and strength. Understanding the effects of these parameters on deposit removal effectiveness is necessary in order to devise more effective sootblowing strategies. Most research on fouling in various boilers [1-6] has focused on measuring and modeling deposit formation and growth, and deposit characteristics as a function of factors including fuel characteristics and boiler operating conditions. On the other hand, sootblowing optimization, and more specifically sootblower jet dynamics and jet-tube/deposit interaction, have received far less attention.

Earlier research at the University of Toronto [7-9] focused on sootblower jet dynamics and the different mechanisms by which deposits are removed from boiler tubes by sootblowers. Deposits may be removed by at least four different mechanisms [9] – brittle breakup due to internal stresses, debonding, vibration or tube bending, and thermal shock, of which brittle breakup and debonding are more important as they are thought to remove most deposits. Experiments involving breakup of gypsum deposits by a supersonic jet [9] have shown that brittle deposit breakup is a very rapid process, occurring in less than a second. Two important factors determining the breakup of brittle deposits are the maximum pressure on the deposit surface produced by the sootblower jet, and the deposit tensile strength. In general, a jet impact pressure of approximately twice the deposit tensile strength is needed to break a deposit.

This paper reviews more recent research done at the University of Toronto on sootblowing optimization [10-13]. The objective of this work was to obtain fundamental information on sootblower jet dynamics and interaction between a sootblower jet, tubes and deposits. We review research activities on three fronts. Investigating the underlying mechanisms by which a sootblower jet interacts with and breaks a deposit will provide insight into how sootblowers should be operated in order to maximize deposit removal. Since this aspect of sootblowing has

not been studied until now, we carried out a large number of lab-scale experiments in which model cylindrical gypsum deposits were exposed to a supersonic air jet; the resulting deposit breakup process was captured using a high speed camera, and analyzed. Second, we visualized the interactions that take place when a supersonic jet impinges onto a single tube as well as a row of tubes. Understanding how a sootblower jet behaves upon impingement on a tube and between tube bundles is important in order to evaluate its operation inside a boiler. Tube bundle geometries (arrangement and spacing) vary with location in different boilers. These tubes pose as obstacles to the jet flow, and may reduce the strength of the jet impinging on the deposits. Consequently flow visualization and strength measurement of the sootblower jet between tube bundles is important. We used the *schlieren* optical technique coupled with high-speed imaging for this purpose. Finally, we present the development of a sootblower jet CFD model, and simulation results that correspond to both laboratory experiments and to experiments conducted in an actual recovery boiler. Numerical modeling of sootblower jets serves two purposes. It provides a means of corroborating experimental results obtained both in the lab and via *in-situ* experiments, and is especially important because these experiments are often difficult to carry out and can be associated with significant uncertainty. The modeling also yields data, such as contours of flow variables including velocity, pressure, density, and turbulence intensity that cannot be obtained experimentally, and so enhances our understanding of the complex phenomena associated with sootblower jets.

2.0 BASIC CONCEPTS AND DEFINITIONS

A sootblower nozzle is designed to operate at a unique steam pressure, the so-called ‘design pressure’. When supplied with steam at that pressure, the supersonic jet that forms downstream of the nozzle exit is said to be ‘full-expanded’, because the jet pressure at the nozzle exit is then equal to the local ambient boiler pressure. A fully-expanded jet consists of a potential core and a turbulent mixing region. In the core region, which usually extends 10-15 nozzle exit diameters downstream of the nozzle exit, the flow properties remain almost unchanged, as illustrated in Figure 1. From a sootblowing perspective, the core of a jet is associated with maximum deposit removal effectiveness, and the core length yields a measure of the distance downstream of the nozzle in which the sootblower jet is most effective.

The core diameter is initially the same as the nozzle exit diameter, but decreases with distance downstream as ambient gas is entrained by the jet; by the end of the core, the entrained fluid has reached the jet centerline. At the same time the overall jet diameter increases with distance from the nozzle, as shown in Figure 1 by the arrows that represent the axial velocity vectors. The local jet diameter can be estimated using the theory and semi-empirical relations presented in [7].

When the supply pressure is different than the design pressure for a given nozzle, the resulting supersonic jet is said to be ‘off-design’ because the local jet pressure at the nozzle exit will be lower or higher than the local ambient boiler pressure; the resulting jets are referred to as over- and under-expanded, respectively. Off-design jets are characterized by a multi-cell shock structure downstream of the nozzle exit that consists of shock and expansion waves. This wave structure is associated with a fluctuating jet pressure, that is the means by which the jet adjusts to the surrounding pressure. Off-design jets involve very complicated phenomena, because of these

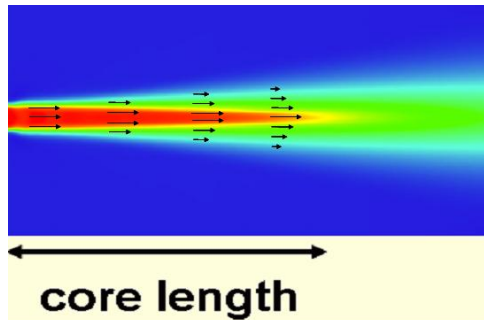


Figure 1: Velocity contours of a free jet (red maximum to blue minimum).

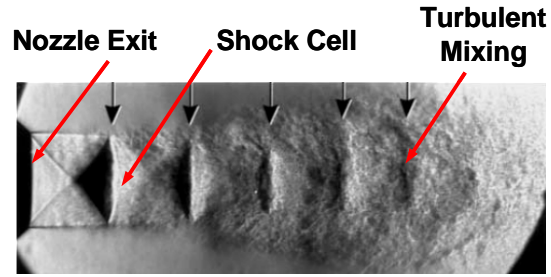


Figure 2: Flow visualization of an off-design supersonic jet (by Panda [14]); Note the shock-cell structure in the flow.

shock waves. Figure 2 is a flow visualization of an off-design jet [14] that nicely illustrates the shock-cell structure and its decay due to turbulent mixing.

Finally, it should be noted that sootblower jet effectiveness has for a long time been correlated with a jet Peak Impact Pressure (PIP), the pressure that would be measured by a pitot tube inserted axially along a jet centerline, because it represents the pressure that a sootblower jet can exert on a deposit. PIP remains constant inside the core of a fully-expanded jet, and then decays further downstream; the PIP measured in an off-design jet will fluctuate before decaying.

3.0 BRITTLE DEPOSIT BREAKUP BY SUPERSONIC JET IMPINGEMENT

The objective of this work was to visualize the failure behaviour of cylindrical brittle deposits impacted by a supersonic air jet, in order to (1) identify different deposit breakup mechanisms, and (2) quantify the effects of different parameters on the breakup process.

3.1 Experimental Apparatus and Procedure

Figure 3a illustrates the experimental apparatus. Compressed air was delivered to a supersonic nozzle (exit diameter, $d_{\text{exit}}=0.74$ cm, a $\frac{1}{4}$ scaled-down version of a typical sootblower nozzle) via a solenoid valve. The supply pressure was set to yield a fully expanded supersonic jet with a nozzle exit Mach number of 2.5, similar to sootblower jets used in kraft recovery boilers. We used gypsum to prepare model deposits, because gypsum is a hard, porous, and brittle material, similar to the majority of deposits in kraft recovery boilers. Moreover, the physical properties (tensile strength and porosity) of gypsum can be controlled by controlling the ratio of water to plaster of Paris when making the gypsum slurry. Cylindrical deposits of 1.27 cm ('thin') and 1.91 cm ('thick') outer diameter (d_{deposit}) were placed at various distances (5, 9, 12, 15 cm) from the nozzle exit, normal to the centerline of the jet. An air jet then impinged on a deposit, and the resulting breakup process was captured from both the front and back sides of the deposit using two synchronized high-speed cameras (4000 frames/s). For each set of experimental parameters, we repeated the breakup tests several times. Also, since actual deposits are not symmetric, the effect of deposit asymmetry on breakup was also investigated. Asymmetric deposits were

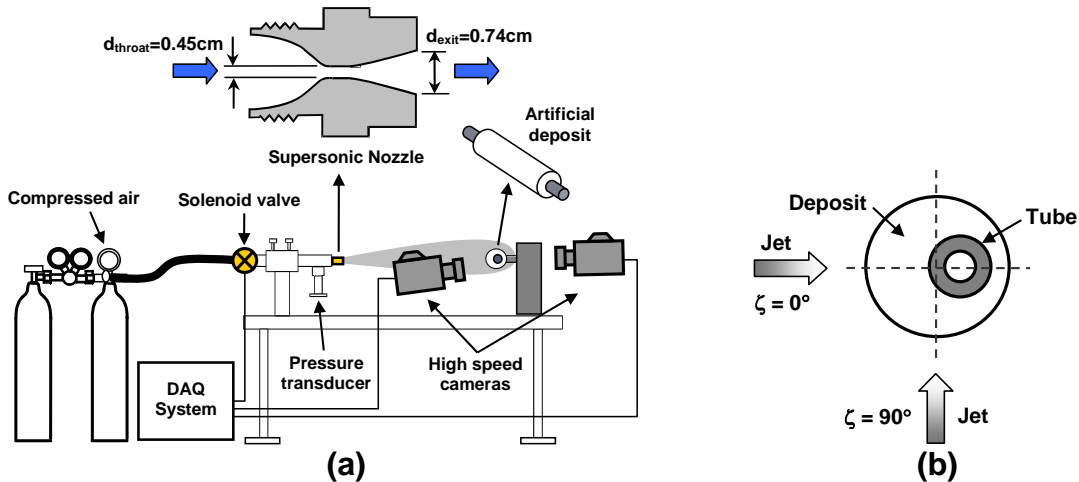


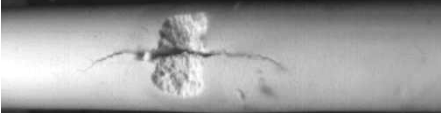
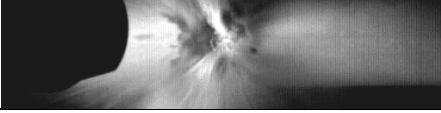
Figure 3: (a) Experimental setup for the brittle deposit breakup tests; (b) orientation angle ζ for asymmetric deposits [11].

prepared by shifting the tube slightly off the longitudinal axis of the deposit, as shown in Figure 3b. Jets were then directed both onto the thickest part of the deposit (orientation angle $\zeta = 0^\circ$), and between the thinnest and thickest parts ($\zeta = 90^\circ$).

3.2 Failure Mechanisms of Deposits: The Importance of Crack Formation

We analyzed the deposit breakup images and movies in detail, and identified three deposit breakup mechanisms - (1) axial crack formation, (2) surface erosion followed by axial crack formation, and (3) surface erosion followed by spalling. Typical images of each mechanism are shown in Table 1. These mechanisms were found to correlate with $d_{jet}/d_{deposit}$. Hence, for deposits placed further from the nozzle (larger values of $d_{jet}/d_{deposit}$), the jet has spread enough to envelope the entire deposit (due to Coanda effect [15]), although the jet PIP has decreased. This creates a pressure distribution around the deposit surface which induces tensile stresses in the deposit. The jet PIP combined with these tensile stresses causes a deep axial crack to form in the deposit. As a result, axial crack formation was observed for larger values of $d_{jet}/d_{deposit}$.

Table 1: Brittle deposit breakup mechanisms.

| Observed Breakup Mechanism | Jet-to-deposit Diameter Ratio | Breakup Image |
|---|-------------------------------------|--|
| Axial crack formation | $d_{jet}/d_{deposit} > 0.51$ |  |
| Surface erosion + axial crack formation | $0.36 < d_{jet}/d_{deposit} < 0.51$ |  |
| Surface erosion + spalling | $d_{jet}/d_{deposit} \leq 0.36$ |  |

When deposits are placed closer to the nozzle, the jet diameter remains almost the same size as the nozzle exit (smaller values of $d_{jet}/d_{deposit}$). The jet is strong and so focuses on a small area of the deposit. Conditions for failure only exist in the vicinity of that stagnation region. As a result, the jet initially drills into the deposit, until conditions become favorable for crack formation. This is observed more for thick deposits than thin ones.

Figure 4a presents a sequence of images of a thin deposit that breaks by axial crack formation; Figure 4b shows the breakup of a thick deposit by surface erosion followed by axial crack formation. Time $t = 0$ marks the onset of breakup of the deposit after the air jet has reached the deposit surface. Axial cracking leads to the breakup of both deposits, but the crack forms much more quickly in the thin deposit, while the thick deposit shows significant surface erosion prior to crack formation. Whereas the time to crack formation is very different, once the axial crack forms, it takes almost the same time for the deposit to be completely removed (about 2-3 ms). This is because cracks propagate within a solid material at the speed of sound, which is on the order of a few thousand metres per second for ceramics. Hence, the difference in size of the two deposits has a negligible effect on the subsequent breakup duration: once cracks form within a deposit, it takes only a little additional time for deposit removal. Hence, it is very important that deep cracks form rapidly when a sootblower jet impinges a deposit, for the deposit to be removed within the short duration it is exposed to the jet.

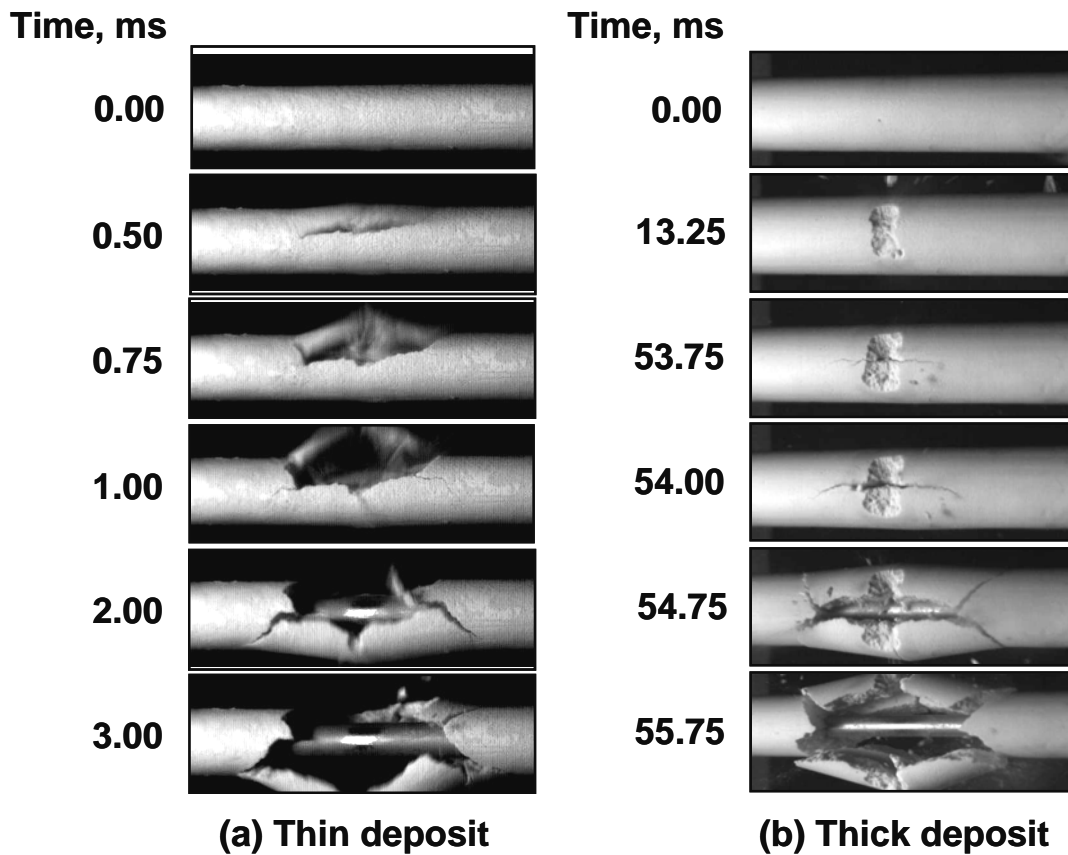


Figure 4: Breakup images of (a) thin [11] and (b) thick deposits placed 9 cm from the nozzle.

3.3 Effects of Other Parameters on the Breakup Process

To quantify the effects of other parameters on the deposit breakup process, three measures of breakup are defined – (1) the pre-breakup duration, which is the time from when the jet first reaches the deposit surface to when the first signs of deposit removal are evident; (2) the breakup duration, which is the time required for the deposit to break once breakup starts; and (3) the breakup length, which is a measure of the amount of deposit removed. Effects of the following parameters on the breakup process were investigated: distance between nozzle and deposit, deposit size, deposit asymmetry, deposit strength, jet duration (exposure time of deposit to jet), and jet attack angle [10, 11].

Figure 5 shows the effects of nozzle-deposit distance, deposit size and deposit asymmetry on the breakup parameters. At large distances away from the nozzle, both the pre-breakup and breakup durations of thick deposits are greater than those of thin ones. Also note that the breakup length of thick asymmetric deposits is greater than the other cases; this is because in the asymmetric orientation, the thickness of the deposit on some parts of the tube is very small. This facilitates rapid cracking and removal of the thinner portion of the deposit first, followed by the remainder of the deposit.

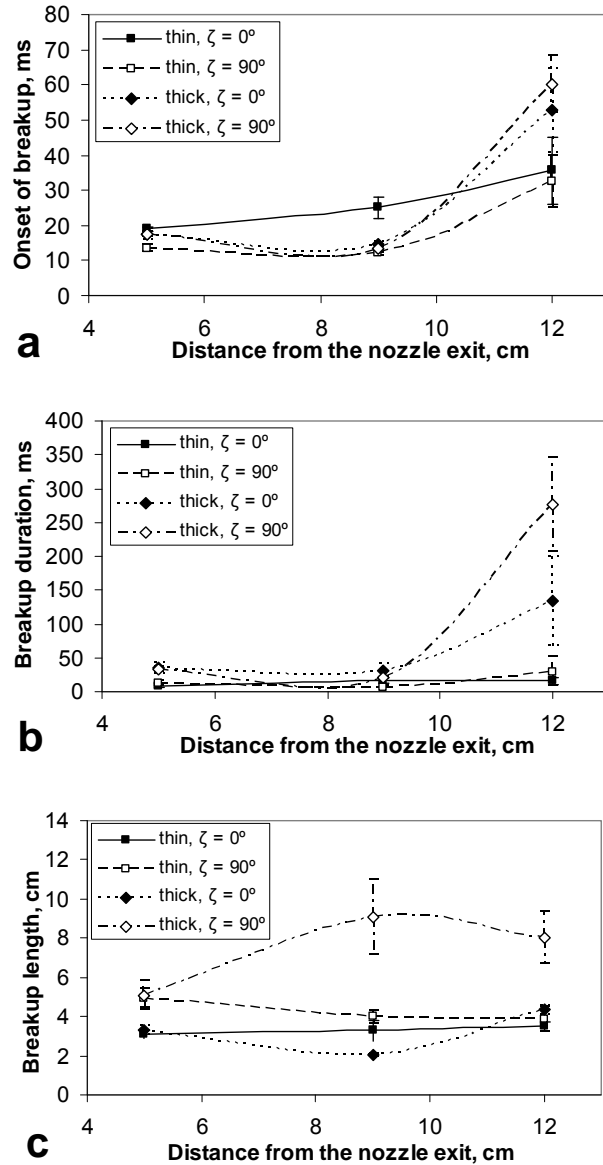


Figure 5: Effects of nozzle-deposit distance, deposit size, and deposit asymmetry on (a) the pre-breakup duration, (b) the breakup duration, and (c) the breakup length [10].

4.0 VISUALIZATION OF A SUPERSONIC JET IMPINGING ON SINGLE AND MULTIPLE TUBES

Sootblower jets cannot be seen by the naked eye, and so a special optical technique is required to visualize them. Taking advantage of the strong density gradients present in these jets (which lead

to refractive index gradients in the jet fluid), the schlieren technique uses parallel (collimated) light to make these refractive index gradients visible. This technique was coupled with high-speed imaging to visualize the interaction between a supersonic jet and single tubes of different sizes (to simulate tubes with deposits) and a row of tubes (to simulate a platen).

4.1 Methodology

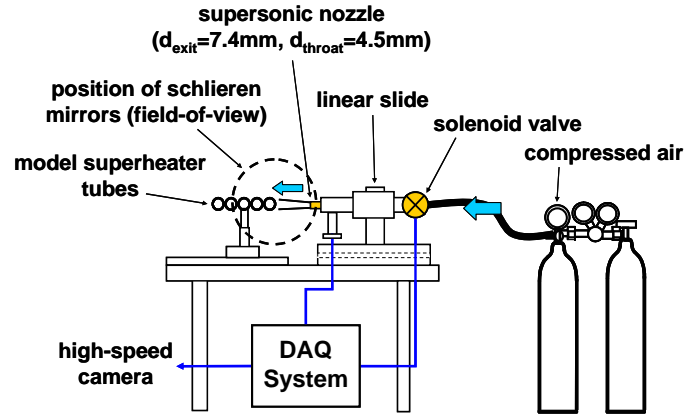


Figure 6: Apparatus for schlieren visualization of jet impingement [13].

The same apparatus used for the deposit breakup experiments was also used for these experiments, except that the gypsum deposits were replaced by steel tubes of different sizes, and the schlieren optical system was added. Figure 6 schematically shows the apparatus and the field-of-view for the schlieren visualization. A supersonic jet dynamically similar to an actual sootblower jet was directed at a steel tube placed at various distances from the nozzle. The jet impinged on single tubes (three sizes) and onto a small platen consisting of five tubes welded together. The smallest tube ($d_T = 1.27$ cm, where d_T is the tube outer diameter) was considered ‘clean’, whereas the other two ($d_T = 1.91$ cm and 2.54 cm) were meant to represent increasingly thick deposits. Effects of the following variables on the flow field were investigated: tube size, offset between the tube/platen centreline and the jet centreline, and the distance between the nozzle exit plane and the tube front surface. We used a conventional 2-mirror schlieren optical system to visualize the supersonic jet and its interaction with tubes. A continuous halogen light source was used, and a high-speed camera was operated at 6000 frames/s to record the jet flow field.

4.2 Jet Impingement onto Single Tubes

Figure 7 shows schlieren images of a jet impinging onto three tubes of increasing size. The tubes are positioned at the appropriate scaled-down distance from the nozzle, corresponding to tubes inside an actual kraft recovery boiler. This portion of the jet is within the potential core, hence the jet has a small diameter and is very strong and focused. The multi-cell shock structure of the jet can be seen.

Figure 7a shows that when a jet impinges a tube, the primary jet terminates in a shock wave (the impingement shock), and two small secondary jets form (the lower secondary jet is hidden by the tube stand). These jets form because the primary jet is supersonic, the tube is located in the high velocity, turbulence-free core of the jet, and the jet size is comparable to the tube size. As the jet size relative to the tube size decreases (Figures 7b and 7c), the secondary jets cease to separate from the tube surface, and a weaker flow attached to the surface develops around the tubes. This implies that a sootblower jet impinging on a big, hard deposit will not form secondary jets.

4.3 Jet Impingement onto a Single Platen

To qualitatively assess the interactions between a tube platen and a sootblower jet, a supersonic jet was directed at a scaled-down platen, varying the offset between the jet and platen centerlines (0 offset implies head-on impingement). Figure 8 shows images of the primary jet impinging the platen. The images clearly show that the intensity and direction of propagation of the secondary jet which forms upon impingement vary with offset, and that a small change in offset can cause a substantial change in the intensity and direction of propagation of the jet. We can see that, as the interaction between the primary jet and the first tube of the platen becomes stronger (from image *g* to *a*), the strength of the secondary jet decreases and its deviation from the original flow direction increases. Consequently, there is little or no jet flow at all beyond the third or fourth tube in the platen. This implies that, when sootblowing between boiler tube platens, there is little or no jet flow beyond the first few tubes of a platen whenever there is some interaction between the jet and the first tube of that platen. Hence, any deposits beyond this point do not experience the sootblower jet for a significant amount of time. These are deposits clinging to the sides of the platens, blocking the flue gas passage. It should also be noted that the secondary jet is so short that it likely will not reach the adjacent platen to possibly clean deposits there.

Figure 8 shows another interesting phenomenon: once the jet is only a small distance from the platen, interaction between the jet and the platen ceases to occur. Images *g* and *h* show that beyond an offset of only about 1.2 cm, there is no jet/platen interaction. This is because of the very low spreading rate of a supersonic jet; it diffuses very little in the core region. As a result, deposits clinging to the side of a platen are not exposed to the sootblower jet, and hence will not be removed. Furthermore, much of the steam that a sootblower blows between platens is wasted, as small offsets are required for interaction to occur between the jet and deposits, and any sootblowing strategy should take this into consideration.

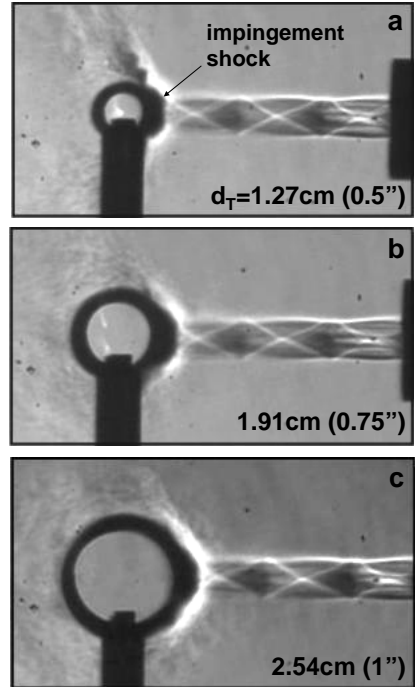


Figure 7: Effect of tube size on jet-tube interaction [13].

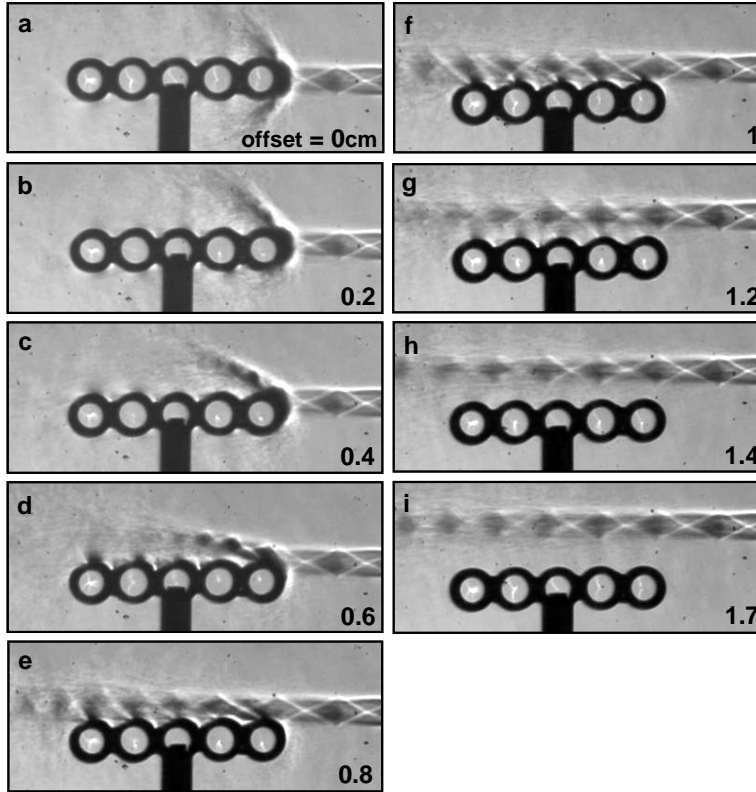


Figure 8: Jet impinging a platen at different offset values [13].

5.0 NUMERICAL MODELING OF SOOTBLOWER JETS

5.1 Model Development

The original CFDLib code obtained from the Los Alamos National Laboratory includes an implementation of the standard $k-\varepsilon$ turbulence model, but does not yield accurate predictions even of relatively simple fully-expanded high speed jets characteristic of sootblowers. Over several years, we have modified the turbulence model by adding compressibility corrections [16] that yielded much better agreement with select measurements of fully-expanded free jets and jet flows between platens; we refer to this model as the SJT (Sootblower Jet Turbulence) model. This model was also validated against a wide range of available experimental data related to fully-expanded free jets and jets impinging on solid surfaces (that lead to the formation of normal shock waves ahead of the surface, characteristic of supersonic flow), and successfully predicted all cases. Figure 9, for example, illustrates the axial velocity, u , versus the axial distance from the nozzle exit, x , along the centerline of a fully-expanded jet, compared to the experimental data of Panda and Seasholtz [17]. The simulation predicts the measurements reasonably well, and illustrates the typical characteristics of a fully-expanded jet: a relatively constant flow for a distance of about 10 nozzle diameters downstream of the nozzle exit (this is the core of the jet, in which the flow properties remain relatively constant), followed by a region in which the velocity decays as the surrounding fluid that is entrained by the jet finally reaches the jet centerline.

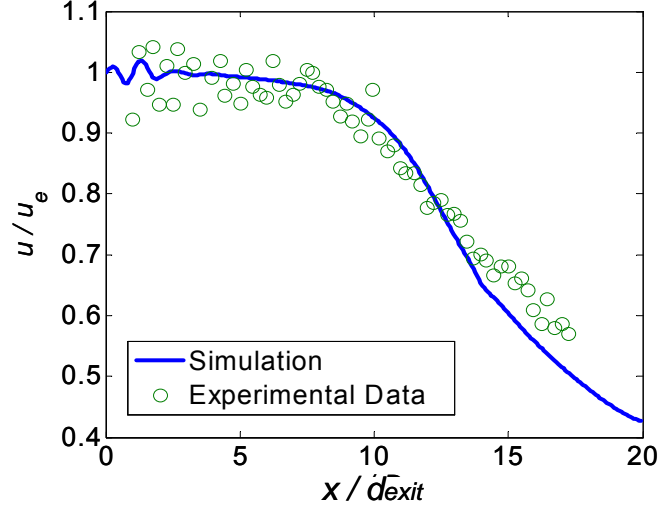


Figure 9: Distribution of the axial velocity along the centerline of a free supersonic jet: comparison of simulation results with the experimental data of Panda and Seasholtz [17]. u_e and d_{exit} represent the nozzle exit velocity and diameter, respectively.

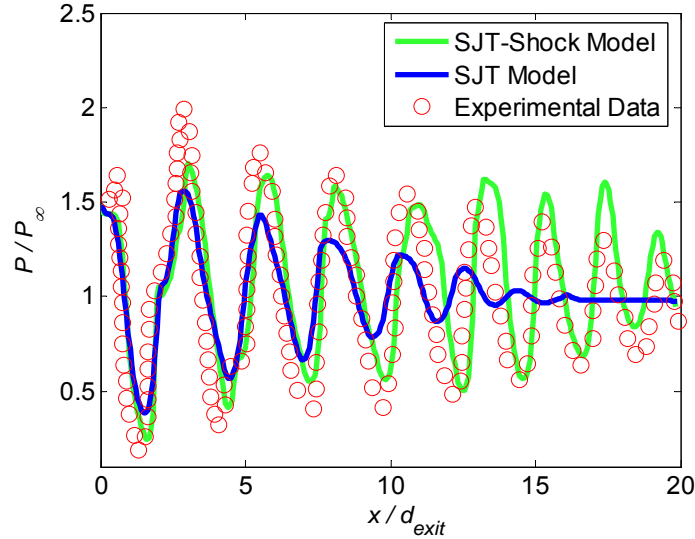


Figure 10. Normalized pressure along the centerline of an off-design jet. P_∞ represents the ambient pressure. Experimental data is that of Norum and Seiner [21].

Accurate simulation of off-design jets, on the other hand, required further corrections, to capture the complex interaction of turbulence and the shock-cell structure that is characteristic of such jets. By imposing a realizability condition [18], and taking into account shock unsteadiness effects [19], an improved turbulence model was developed [20]. The improved model, referred to as the SJT-Shock model, yielded much better agreement with experimental data of off-design jets. Figure 10 presents predictions of centerline pressure versus axial distance from the nozzle exit for an off-design jet, obtained using the SJT and SJT-Shock models, and compares the results with the experimental data of Norum and Seiner [21]. The results are very different from those presented in Figure 9, in that the pressure even within the core of the jet oscillates strongly as the flow compresses and expands, as it adjusts to the ambient pressure via the shock-cell structure. As can be seen, the SJT model predicts the positions of the first few waves correctly, but

dramatically under-predicts the amplitudes of the waves, which decay much more rapidly than they should. The SJT-Shock model, on the other hand, yields a much better agreement with the experimental data, by limiting the rate of dissipation of the jet.

5.2 Predictions of Actual Sootblower Force

Finally, the SJT-Shock model was used to simulate data measured during a series of tests carried out at the SCA Obbola kraft pulp mill in Sweden [22]. The experiments measured the force exerted by an actual sootblower jet on a circular probe, 4.8 cm in diameter, positioned between two tube banks in a recovery boiler. A detailed description of the experimental setup and of the data that was collected is in [22]. Two tests were carried out: during the first test, the boiler was not operating and steam for the sootblower was delivered from another boiler; for the second test, the boiler was operational. The first set of measurements was obtained for lance pressures of 4, 6, 8, 10 and 12 bars (gauge). During the second test, the lance pressures fluctuated somewhat and so the lance pressures were characterized as 10-11, 13-15 and 17-18 bars (gauge). The design lance pressure for the sootblower nozzles installed in the boiler was about 11 bars (gauge), and so all of the jets were at least somewhat off-design.

Simulations were run using the SJT-Shock model to predict the measured forces, although the properties of air were used instead of steam, and the tube banks were approximated as platens, as shown in Figure 11. These simplifications are unlikely to have had a significant effect on the computed results. The predicted force exerted by the jet on the probe was then calculated by integration of the PIP over the circular region corresponding to the front plate of the measuring probe (i.e. a circle of diameter 48 mm).

Figure 12 shows simulation and test results obtained at lance pressures of 8 bars (top) and 17-18 bars (bottom). The simulation results are in surprisingly good agreement with the measurements, given the complexity of the experiments and the uncertainty associated with the data. It is important to appreciate that these results are an integration of data over a region that encompasses flow within 24 mm off the centerline of the jet; this smooths the fluctuations in pressure associated with an off-design jet. It is useful to note the difference between behaviors of PIP and force exerted by a sootblower jet. As was discussed, PIP and other flow properties vary little in the jet core, i.e. within 10-15 nozzle exit diameters downstream of the nozzle. Force, on the other hand, decreases dramatically, beginning almost immediately downstream of the nozzle exit, as can be seen in Figure 12. The reason is that the jet core shrinks almost linearly in the radial direction with distance from the nozzle exit, as was discussed in Section 2. Because the cross section area of the core shrinks linearly, while PIP remains unchanged in the core, the force exerted by the jet decreases more or less linearly in the core region. The results clearly illustrate the very limited distance over which a sootblower jet exerts appreciable force.

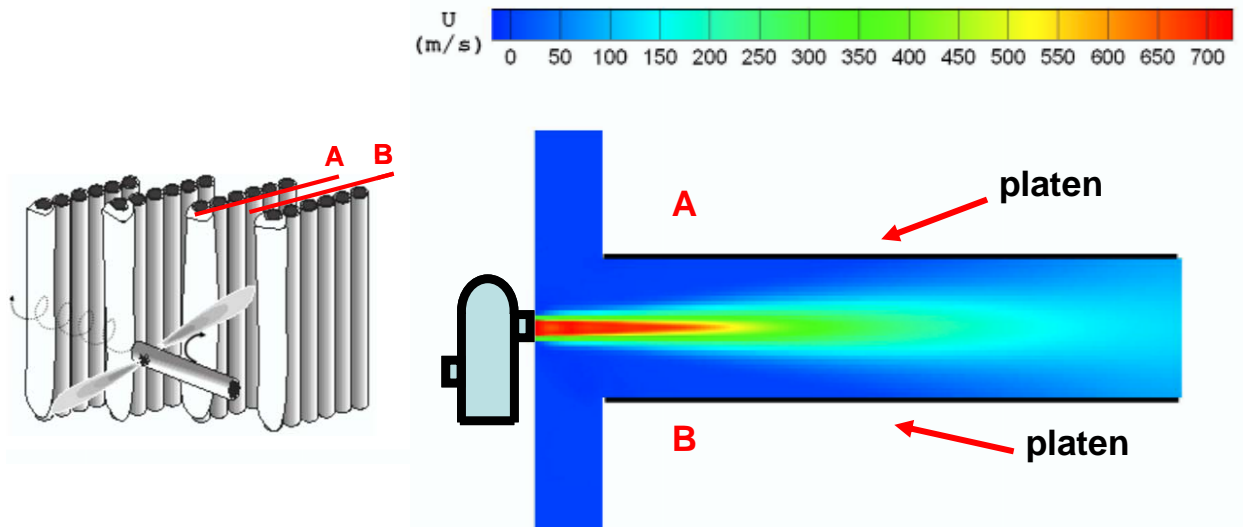


Figure 11. Schematic view of a sootblower jet between superheater platens (left), an axial velocity contour from the simulation (right).

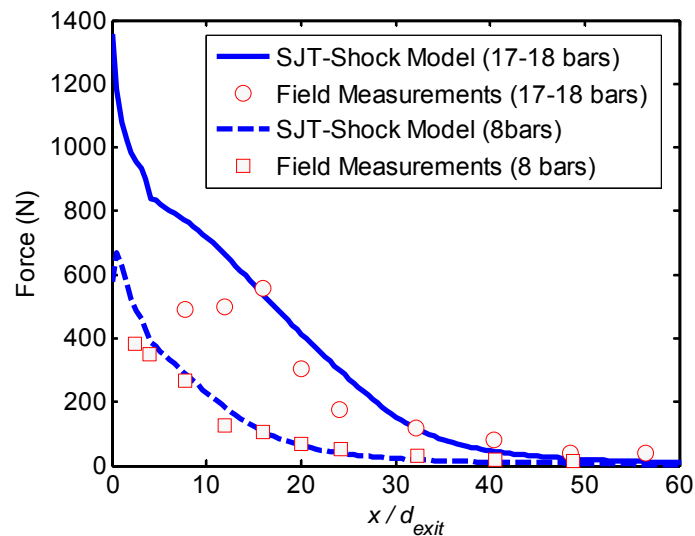


Figure 12. Results for lance pressures of 8 and 17-18 bars (gauge). Nozzle exit diameter, $d_{exit} = 3.7$ cm.

6.0 SUMMARY

This paper has reviewed recent research conducted at the Pulp and Paper Centre at the University of Toronto, on the removal of fireside deposits in boilers by sootblowers. The focus was on obtaining a better understanding of sootblower jet dynamics, and the interaction between sootblower jets and boiler tubes and deposits. These objectives were met by adopting three approaches – studying brittle deposit breakup by high-speed gas jet impingement, visualizing the

interactions between a supersonic jet and single and multiple tubes, and numerical modelling of fully-expanded and off-design sootblower jets.

In the work on brittle deposit breakup, model brittle deposits were impinged by a supersonic air jet under different operating conditions, and the resulting breakup process was captured by high-speed cameras. Three different deposit breakup mechanisms were identified and found to correlate with the jet-to-deposit diameter ratio. It was found that formation of deep cracks in deposits is vital for fast breakup. Cracks form easily and quickly in thin deposits, whereas in thick deposits, crack formation can only occur after the jet has drilled a hole into the deposit.

Schlieren images of the interaction between a supersonic jet and single and multiple tubes revealed the formation of a small, secondary supersonic jet; its intensity and direction of propagation changes continuously with the extent of interaction between the primary jet and tubes. The results imply that whenever there is any interaction between the jet and the first tube of a platen, that there is little sootblower jet flow beyond the third or fourth tubes. Hence, any deposits beyond this point do not experience the sootblower jet for any significant amount of time. Results also showed that the sootblower jet must be directed very close to a platen for any interaction to occur.

Finally, a CFD model has been developed to accurately predict the flow physics of a turbulent supersonic sootblower jet, by incorporating various corrections into a standard turbulence model. The model yields accurate predictions for a wide range of flow behavior, from fully-expanded jets to the much more complicated off-design jets that are characterized by multi-cell shock structures. The model has been validated by comparison with experimental data obtained in our own lab and data available in the scientific literature, and by comparison with data obtained via tests conducted in an actual boiler. The predictions are in some cases surprisingly good, given the uncertainty associated with some of the data, and demonstrate that the model is well-suited to predict a wide range of sootblower jet behavior.

7.0 REFERENCES

- [1] Tran, H. N., TAPPI 1992 Kraft Recovery Boiler Operation Short Course, p. 209, TAPPI PRESS, Atlanta (1992).
- [2] Raask, E., Mineral Impurities in Coal Combustion, Hemisphere, 1985.
- [3] Baxter, L. L., Abbott, M. F., and Douglas, R. E. In S. A. Benson (Ed.), Inorganic Transformations and Ash Deposition during Combustion, Engineering Foundation Meeting, New York, 1992.
- [4] Erickson, T. A., Allan, S. E., McCollor, D. P., Hurley, J. P., Srinivasachar, S., Kang, S. G., Baker, J. E., Morgan, M. E., Johnson, S. A., and Borio, R., Modeling of fouling and slagging in coal-fired utility boilers, Fuel Processing Technology, 44, pp. 155-171, 1995.
- [5] Jenkins, B. M., Baxter, L. L., Miles Jr., T. R., and Miles, T. R., Combustion properties of biomass, Fuel Processing Technology, 54, pp. 17-46, 1998.
- [6] Romeo, L. M. and Garetta, R., Fouling control in biomass boilers, Biomass and Bioenergy, 33, pp. 854-861, 2009.

- [7] Jameel, M. I., Cormack, D. E., Tran, H. N., and Moskal, T. E., Sootblower Optimization - Part 1: Fundamental Hydrodynamics of a Sootblower Nozzle and Jet, TAPPI Journal, 77(5), pp. 135-142, 1994.
- [8] Kaliazine, A. L., Cormack, D. E., Ebrahimi-Sabet, A., and Tran, H. N., The Mechanics of Deposit Removal in Kraft Recovery Boilers, Journal of Pulp and Paper Science, 25(12), pp. 418-424, 1999.
- [9] Kaliazine, A. L., Piroozmand, F., Cormack, D. E., and Tran, H. N., Sootblower Optimization Part II: Deposit and sootblower interaction, TAPPI Journal, 80(11), pp. 201-207, 1997.
- [10] Eslamian, M., Pophali, A., Bussmann, M., and Tran, H. N., Breakup of brittle deposits by supersonic air jet: The effects of varying jet and deposit characteristics, International Journal of Impact Engineering, 36(2), pp. 199-209, 2009.
- [11] Pophali, A., Eslamian, M., Kaliazine, A., Bussmann, M., and Tran, H. N., Breakup mechanisms of brittle deposits in kraft recovery boilers – a fundamental study, TAPPI Journal, 8(9), pp. 4-9, 2009.
- [12] Kaliazine, A., Eslamian, M., and Tran, H. N., On the failure of a brittle material by high velocity gas jet impact, International Journal of Impact Engineering, 37(2), pp. 131-140, 2010.
- [13] Pophali, A., Bussmann, M., and Tran, H. N., Visualizing the Interactions between a Sootblower Jet and a Superheater Platen, In Proceedings of the 2010 International Chemical Recovery Conference, Mar. 29-Apr. 1, Williamsburg, VA, 2010.
- [14] Panda, J., Shock Oscillation in Underexpanded Screeching Jets, Journal of Fluid Mechanics, 363, pp. 173-198, 1998.
- [15] Brahma, R. K., Faruque, O., and Arora, R. C., Experimental investigation of mean flow characteristics of slot jet impingement on a cylinder, Wärme- und Stoffübertragung, 26, pp. 257-263, 1991.
- [16] Tandra, D. S., Development and Application of a Turbulence Model for a Sootblower Jet Propagating between Recovery Boiler Superheater Platens, PhD Thesis, Department of Chemical Engineering and Applied Chemistry, University of Toronto, 2005.
- [17] Panda J., and Seasholtz R. G., Velocity and temperature measurement in supersonic free jets using spectrally resolved Rayleigh scattering, AIAA Paper 99-0296, 1999.
- [18] Thivet, F., Knight, D.D., and Zheltovodov, A.A., Importance of Limiting the Turbulent Stresses to Predict 3D Shock Wave/Boundary Layer Interactions, 23rd Symposium on Shock Waves, Paper No. 2761, 2001.
- [19] Sinha, K., Mahesh, K., and Candler, G.V., Modeling the Effect of Shock Unsteadiness in Shock/Turbulent Boundary-Layer Interactions, AIAA Journal, 43, No. 3, pp. 586-594, 2005.
- [20] Emami B., Numerical Simulation of Kraft Recovery Boiler Sootblower Jets, PhD Thesis, Department of Mechanical and Industrial Engineering, University of Toronto, 2009.
- [21] Norum, T. D., and Seiner, J. M., Measurements of mean static pressure and far-field acoustics of shock containing supersonic jets, NASA Technical Memorandum 84521, 1982.
- [22] Saviharju, K., Kaliazine, A., Tran, H. N., Habib, T., In-situ measurements of sootblower jet impact in a recovery boiler, TAPPI/PAPTAC International Chemical Recovery Conference, Williamsburg, VA, March 2010.